Viscous dissipation as a mechanism for spatiotemporal chaos in Rayleigh-Bénard convection between poorly conducting boundaries at infinite Prandtl number

Leonid Kagan [1,*] Peter V. Gordon, [2,†] and Gregory Sivashinsky [1,‡]
[1] School of Mathematical Sciences, Tel Aviv University, Tel Aviv 69978, Israel
[2] Department of Mathematical Sciences, Kent State University, Kent, Ohio 44242, USA

(Received 7 August 2022; accepted 24 October 2022; published 9 November 2022)

Nonlinear Rayleigh-Bénard convection in an infinite-Prandtl-number fluid layer between poorly conducting boundaries is considered as a model for convection in the earth's upper mantle. It is shown that accounting for the generally neglected impact of viscous dissipation may lead to the development of large-scale spatiotemporal chaotic dynamics governed by the familiar Kuramoto-Sivashinsky equation $\Phi_\tau + \nabla^4\Phi + 2\nabla^2\Phi - (\nabla\Phi)^2 + \alpha\Phi = 0$, known to occur in various physical systems.

DOI: 10.1103/PhysRevFluids.7.113501

I. PROBLEM STATEMENT AND BASIC EQUATIONS

The problem of buoyancy-induced convection in horizontal layers of fluid heated from below traditionally neglects the internal heating induced by viscous dissipation. However, it has long been observed that viscous dissipations may be important if the width of the layer is large enough. Such might be the case of convection of the earth's mantle [1], where the dissipation number Di [see Eq. (1) below] is of the order of unity. As shown below, close to the stability threshold, viscous dissipation may trigger a nonrelaxational irregular spatiotemporal evolution of convective cells. To demonstrate the effect we consider the case of nearly insulating boundaries (relevant to mantle convection [2–4]) where the longitudinal dimension of convective cells is significantly greater than the layer's thickness. This allows separation of horizontal and vertical spatial variables, thus lowering the effective dimensionality of the problem [2,3,5,6].

Except for the viscous dissipation term, the model employed is closely parallel to the seminal formulation of Rayleigh [7] (see also Refs. [2–6,8]), pertinent to the Newtonian fluid with constant transport coefficients and the Boussinesq distinguished limit. In suitably selected nondimensional variables, the model may be formulated as follows. The heat equation

$$\frac{\partial\theta}{\partial t} + \frac{\partial u\theta}{\partial x} + \frac{\partial v\theta}{\partial y} + \frac{\partial w\theta}{\partial z} - w = \frac{\partial^2\theta}{\partial x^2} + \frac{\partial^2\theta}{\partial y^2} + \frac{\partial^2\theta}{\partial z^2} + \frac{\mathrm{Di}}{\mathrm{Ra}}\phi, \tag{1}$$

where ϕ is the dissipation rate

$$\phi = 2\left[\left(\frac{\partial u}{\partial x}\right)^2 + \left(\frac{\partial v}{\partial y}\right)^2 + \left(\frac{\partial w}{\partial z}\right)^2\right] + \left(\frac{\partial u}{\partial y} + \frac{\partial v}{\partial x}\right)^2 + \left(\frac{\partial u}{\partial z} + \frac{\partial w}{\partial x}\right)^2 + \left(\frac{\partial v}{\partial z} + \frac{\partial w}{\partial y}\right)^2. \tag{2}$$

*Corresponding author: kaganleo@tauex.tau.ac.il
†gordon@math.kent.edu
‡grishas@tauex.tau.ac.il

Having the earth's mantle convection in mind, the Prandtl number is regarded as infinitely high [2–5]. As a result, the momentum equations become

$$\frac{\partial p}{\partial x} = \frac{\partial^2 u}{\partial x^2} + \frac{\partial^2 u}{\partial y^2} + \frac{\partial^2 u}{\partial z^2}, \tag{3}$$

$$\frac{\partial p}{\partial y} = \frac{\partial^2 v}{\partial x^2} + \frac{\partial^2 v}{\partial y^2} + \frac{\partial^2 v}{\partial z^2}, \tag{4}$$

$$\frac{\partial p}{\partial z} = \frac{\partial^2 w}{\partial x^2} + \frac{\partial^2 w}{\partial y^2} + \frac{\partial^2 w}{\partial z^2} + \mathrm{Ra}\theta. \tag{5}$$

The continuity equation

$$\frac{\partial u}{\partial x} + \frac{\partial v}{\partial y} + \frac{\partial w}{\partial z} = 0. \tag{6}$$

Equations (1)–(6) are considered in the layer

$$-\infty < x, y < \infty, \quad 0 < z < 1.$$

For the case of a liquid layer between two rigid plates, the boundary conditions at $z = 0$, 1 read

$$u(z = 0, 1) = v(z = 0, 1) = w(z = 0, 1) = 0, \tag{7}$$

$$\frac{\partial \theta(z = 0)}{\partial z} = \mathrm{Bi}_b\theta, \quad \frac{\partial \theta(z = 1)}{\partial z} = -\mathrm{Bi}_t\theta. \tag{8}$$

To exclude the convective flow total expenditure, the model is augmented with an additional long-time condition for a well-settled (yet generally unsteady) flow,

$$\int_0^1 u\, dz = \int_0^1 v\, dz = 0. \tag{9}$$

This condition is particularly transparent for the two-dimensional version of the problem, where the flow velocity may be described in terms of the stream function: $u = -\partial\Psi/\partial z$, $v = 0$, and $w = \partial\Psi/\partial x$. Equation (9) then readily implies $\Psi(z = 0, 1) = 0$ [2,5].

The following notation was used in Eqs. (1)–(8): θ is the nondimensional temperature disturbance in units of the difference between the temperature of the bottom (T_-) and that of the upper boundary (T_+) in the absence of convection; x, y, z, and t are the nondimensional space and time coordinates in units of the thickness d of the liquid layer and the time interval d^2/κ, respectively; κ is the thermal diffusivity of the liquid; u, v, w, and p are the nondimensional flow velocities and pressure in units of κ/d and κ/d^2, respectively; $\mathrm{Ra} = \sigma g(T_- - T_+)d^3/\nu\kappa$ is the Rayleigh number; σ is the volume expansion coefficient; g is the gravitational acceleration; ν is the kinematic viscosity; $\mathrm{Pr} = \nu/\kappa$ is the Prandtl number; $\mathrm{Di} = \sigma g d/c_p$ is the dissipation number; c_p is the specific heat at constant pressure; and Bi_b and Bi_t are the nondimensional coefficients of heat exchange between the liquid and boundaries (Biot numbers).

II. ASYMPTOTIC ANALYSIS

Let the Rayleigh number be close to the critical value Ra_c, corresponding to the onset of convection,

$$\mathrm{Ra} = \mathrm{Ra}_c(1 + \varepsilon) \quad (\varepsilon \ll 1). \tag{10}$$

Assuming the heat loss to be small [5,6,8],

$$\mathrm{Bi}_b = \varepsilon^2\beta_b, \quad \mathrm{Bi}_t = \varepsilon^2\beta_t, \tag{11}$$

we introduce the scaled space and time variables

$$\hat{x} = \sqrt{\varepsilon}x, \quad \hat{y} = \sqrt{\varepsilon}y, \quad \hat{z} = z, \quad \hat{t} = \varepsilon^2 t. \tag{12}$$

This choice of scalings is dictated by the results of the linear stability analysis [2,5]. Assuming the dissipation number Di to be of the order of unity, we introduce new scaled variables $\hat{\theta}$, $\hat{u}$, $\hat{v}$, $\hat{w}$, and $\hat{p}$ for the disturbances of temperature, flow field, and pressure,

$$\theta = \varepsilon\hat{\theta}, \quad u = \varepsilon\sqrt{\varepsilon}\hat{u}, \quad v = \varepsilon\sqrt{\varepsilon}\hat{v}, \quad w = \varepsilon^2\hat{w}, \quad p = \varepsilon\hat{p}. \tag{13}$$

This scaling is suggested by the relations (12) and the requirement of the asymptotic balance between the terms $\partial\theta/\partial t$ and $\partial^2 u/\partial z^2 + \partial^2 v/\partial z^2$ of Eqs. (1) and (2); $\partial p/\partial x$, $\partial p/\partial y$, $\partial^2 u/\partial z^2$, and $\partial^2 v/\partial z^2$ of Eqs. (3) and (4); $\partial p/\partial z$ and θ of Eq. (5); and $\partial w/\partial z$ and $\partial u/\partial x + \partial v/\partial y$ of Eq. (6). In terms of new variables the problem (1)–(9) becomes.

$$\varepsilon^2\frac{\partial\hat{\theta}}{\partial\hat{t}} + \varepsilon^2\frac{\partial\hat{u}\hat{\theta}}{\partial\hat{x}} + \varepsilon^2\frac{\partial\hat{v}\hat{\theta}}{\partial\hat{y}} + \varepsilon^2\frac{\partial\hat{w}\hat{\theta}}{\partial\hat{z}} - \varepsilon\hat{w} = \varepsilon\frac{\partial^2\hat{\theta}}{\partial\hat{x}^2} + \varepsilon\frac{\partial^2\hat{\theta}}{\partial\hat{y}^2} + \frac{\partial^2\hat{\theta}}{\partial\hat{z}^2} + \frac{\mathrm{Di}}{\mathrm{Ra}_c}\left[\varepsilon^2\left(\frac{\partial\hat{u}}{\partial\hat{z}}\right)^2 + \varepsilon^2\left(\frac{\partial\hat{v}}{\partial\hat{z}}\right)^2 + O(\varepsilon^3)\right], \tag{14}$$

$$\frac{\partial\hat{p}}{\partial\hat{x}} = \varepsilon\frac{\partial^2\hat{u}}{\partial\hat{x}^2} + \varepsilon\frac{\partial^2\hat{u}}{\partial\hat{y}^2} + \frac{\partial^2\hat{u}}{\partial\hat{z}^2}, \tag{15}$$

$$\frac{\partial\hat{p}}{\partial\hat{y}} = \varepsilon\frac{\partial^2\hat{v}}{\partial\hat{x}^2} + \varepsilon\frac{\partial^2\hat{v}}{\partial\hat{y}^2} + \frac{\partial^2\hat{v}}{\partial\hat{z}^2}, \tag{16}$$

$$\frac{\partial\hat{p}}{\partial\hat{z}} = \varepsilon^2\frac{\partial^2\hat{w}}{\partial\hat{x}^2} + \varepsilon^2\frac{\partial^2\hat{w}}{\partial\hat{y}^2} + \varepsilon\frac{\partial^2\hat{w}}{\partial\hat{z}^2} + \mathrm{Ra}_c(1+\varepsilon)\hat{\theta}, \tag{17}$$

$$\frac{\partial^2\hat{u}}{\partial\hat{x}} + \frac{\partial^2\hat{v}}{\partial\hat{y}} + \frac{\partial^2\hat{w}}{\partial\hat{z}} = 0, \tag{18}$$

$$\hat{u}(\hat{z}=0,1) = \hat{v}(\hat{z}=0,1) = \hat{w}(\hat{z}=0,1) = 0, \tag{19}$$

$$\frac{\partial\hat{\theta}(\hat{z}=0)}{\partial\hat{z}} = \varepsilon^2\beta_b\hat{\theta}(\hat{z}=0), \qquad \frac{\partial\hat{\theta}(\hat{z}=1)}{\partial\hat{z}} = -\varepsilon^2\beta_t\hat{\theta}(\hat{z}=1), \tag{20}$$

$$\int_0^1 \hat{u}\,d\hat{z} = \int_0^1 \hat{v}\,d\hat{z} = 0. \tag{21}$$

For the subsequent arguments it is useful to integrate Eq. (14) over the interval $0 < \hat{z} < 1$. Noting the boundary conditions (19) and (20), we can write the resulting integral relation as

$$\varepsilon\frac{\partial}{\partial\hat{t}}\int_0^1 \hat{\theta}\,d\hat{z} + \varepsilon\frac{\partial}{\partial\hat{x}}\int_0^1 \hat{u}\hat{\theta}\,d\hat{z} + \varepsilon\frac{\partial}{\partial\hat{y}}\int_0^1 \hat{v}\hat{\theta}\,d\hat{z} - \int_0^1 \hat{w}\,d\hat{z} = \frac{\partial^2}{\partial\hat{x}^2}\int_0^1 \hat{\theta}d\hat{z} + \frac{\partial^2}{\partial\hat{y}^2}\int_0^1 \hat{\theta}d\hat{z} + (\beta_b+\beta_t)\varepsilon[\hat{\theta}(\hat{z}=0) + \hat{\theta}(\hat{z}=1)] + \varepsilon\frac{\mathrm{Di}}{\mathrm{Ra}_c}\int_0^1\left[\left(\frac{\partial\hat{u}}{\partial\hat{z}}\right)^2 + \left(\frac{\partial\hat{v}}{\partial\hat{z}}\right)^2\right]d\hat{z} + O(\varepsilon^2). \tag{22}$$

A solution of the problem (14)–(21) will be sought as an asymptotic expansion

$$\hat{\theta} = \hat{\theta}^{(0)} + \varepsilon\hat{\theta}^{(1)} + \cdots, \quad \hat{u} = \hat{u}^{(0)} + \varepsilon\hat{u}^{(1)} + \cdots, \quad \hat{v} = \hat{v}^{(0)} + \varepsilon\hat{v}^{(1)} + \cdots, \tag{23}$$

$$\hat{w} = \hat{w}^{(0)} + \varepsilon\hat{w}^{(1)} + \cdots, \quad \hat{p} = \hat{p}^{(0)} + \varepsilon\hat{p}^{(1)} + \cdots.$$

The problem (14)–(21) in the zeroth approximation yields

$$\frac{\partial^2\hat{\theta}^{(0)}}{\partial\hat{z}^2} = 0, \quad \frac{\partial\hat{p}^{(0)}}{\partial\hat{x}} = \frac{\partial^2\hat{u}^{(0)}}{\partial\hat{z}^2}, \quad \frac{\partial\hat{p}^{(0)}}{\partial\hat{y}} = \frac{\partial^2\hat{v}^{(0)}}{\partial\hat{z}^2}, \quad \frac{\partial\hat{p}^{(0)}}{\partial\hat{z}} = \mathrm{Ra}_c\hat{\theta}^{(0)}, \quad \frac{\partial\hat{u}^{(0)}}{\partial\hat{x}} + \frac{\partial\hat{v}^{(0)}}{\partial\hat{y}} + \frac{\partial\hat{w}^{(0)}}{\partial\hat{z}} = 0, \tag{24}$$

$$\hat{u}^{(0)}(\hat{z} = 0, 1) = \hat{v}^{(0)}(\hat{z} = 0, 1) = \hat{w}^{(0)}(\hat{z} = 0, 1) = 0, \tag{25}$$

$$\frac{\partial\hat{\theta}^{(0)}(\hat{z} = 0, 1)}{\partial\hat{z}} = 0, \tag{26}$$

$$\int_0^1 \hat{u}^{(0)} d\hat{z} = \int_0^1 \hat{v}^{(0)} d\hat{z} = 0. \tag{27}$$

Hence,

$$\hat{\theta}^{(0)} = F(\hat{x}, \hat{y}, \hat{t}), \quad \hat{u}^{(0)} = \frac{1}{12}\mathrm{Ra}_c\left(\frac{\partial F}{\partial\hat{x}}\right)(2\hat{z}^2 - 3\hat{z} + \hat{z}),$$

$$\hat{v}^{(0)} = \frac{1}{12}\mathrm{Ra}_c\left(\frac{\partial F}{\partial\hat{y}}\right)(2\hat{z}^2 - 3\hat{z} + \hat{z}), \tag{28}$$

$$\hat{w}^{(0)} = -\tfrac{1}{24}\mathrm{Ra}_c\nabla^2 F(\hat{z}^4 - 2\hat{z}^3 + \hat{z}^2),$$

$$\hat{p}^{(0)} = \tfrac{1}{2}\mathrm{Ra}_c F(2\hat{z} - 1), \quad \text{where} \quad \nabla = (\partial/\partial\hat{x}, \partial/\partial\hat{y}).$$

The integral relation (22) for the zeroth approximation yields

$$\int_0^1 \hat{w}^{(0)} d\hat{z} = -\nabla^2 F. \tag{29}$$

Hence, using (28) for $\hat{w}^{(0)}$, we have

$$(\mathrm{Ra}_c - 720)\nabla^2 F = 0, \quad \text{i.e., } \mathrm{Ra}_c = 720. \tag{30}$$

To determine the as yet unknown function $F(\hat{x}, \hat{y}, \hat{t})$, we proceed to the next approximation. In this case the system of equations and boundary conditions are

$$\hat{w}^{(0)} = -\nabla^2 F - \frac{\partial^2\hat{\theta}^{(1)}}{\partial\hat{z}^2}, \tag{31}$$

$$\frac{\partial\hat{p}^{(1)}}{\partial\hat{x}} = \nabla^2\hat{u}^{(0)} + \frac{\partial^2\hat{u}^{(1)}}{\partial\hat{z}^2}, \tag{32}$$

$$\frac{\partial\hat{p}^{(1)}}{\partial\hat{y}} = \nabla^2\hat{v}^{(0)} + \frac{\partial^2\hat{v}^{(1)}}{\partial\hat{z}^2}, \tag{33}$$

$$\frac{\partial\hat{p}^{(1)}}{\partial\hat{z}} = \frac{\partial^2\hat{w}^{(0)}}{\partial\hat{z}^2} + \mathrm{Ra}_c\hat{\theta}^{(1)} + \mathrm{Ra}_c F, \tag{34}$$

$$\frac{\partial \hat{u}^{(1)}}{\partial \hat{x}} + \frac{\partial \hat{v}^{(1)}}{\partial \hat{y}} + \frac{\partial \hat{w}^{(1)}}{\partial \hat{z}} = 0, \tag{35}$$

$$\hat{u}^{(1)}(\hat{z} = 0, 1) = \hat{v}^{(1)}(\hat{z} = 0, 1) = \hat{w}^{(1)}(\hat{z} = 0, 1) = 0, \tag{36}$$

$$\frac{\partial \hat{\theta}^{(1)}}{\partial \hat{z}} = 0,$$

$$\int_0^1 \hat{u}^{(1)} d\hat{z} = \int_0^1 \hat{v}^{(1)} d\hat{z} = 0. \tag{37}$$

Hence, in view of (28) and (30) we have

$$\hat{\theta}^{(1)} = \tfrac{1}{2}\nabla^2 F (2\hat{z}^6 - 6\hat{z}^5 + 5\hat{z}^4 - \hat{z}^2) + G(\hat{x}, \hat{y}, \hat{t}), \tag{38}$$

$$\begin{aligned}\hat{w}^{(1)} = &- \tfrac{1}{14}\nabla^4 F (2\hat{z}^{10} - 10\hat{z}^9 + 15\hat{z}^8 - 42\hat{z}^6 \\ &+ 84\hat{z}^5 - 70\hat{z}^4 + 20\hat{z}^3 + \hat{z}^2) - 30\nabla^2 F(\hat{z}^4 - 2\hat{z}^3 + \hat{z}^2) - 30\nabla^2 G(\hat{z}^4 - 2\hat{z}^3 + \hat{z}^2).\end{aligned} \tag{39}$$

Expressions for $\hat{u}^{(1)}$, $\hat{v}^{(1)}$, and $\hat{p}^{(1)}$ are omitted for brevity.

For the first approximation the integral relationship (22), accounting for (27), yields

$$\begin{aligned}\frac{\partial F}{\partial \hat{t}} - \int_0^1 \hat{w}^{(1)} d\hat{z} = \nabla^2 \int_0^1 \hat{\theta}^{(1)} d\hat{z} - (\beta_b + \beta_t)F \\ + \frac{\mathrm{Di}}{\mathrm{Ra}_c} \int_0^1 \left[\left(\frac{\partial \hat{u}^{(0)}}{\partial \hat{z}} \right)^2 + \left(\frac{\partial \hat{v}^{(0)}}{\partial \hat{z}} \right)^2 \right] d\hat{z}.\end{aligned} \tag{40}$$

Inserting the expressions found above for $\hat{\theta}^{(1)}$, $\hat{u}^{(0)}$, $\hat{v}^{(0)}$, and $\hat{w}^{(1)}$ into (40), we obtain the required equation for $F(\hat{x}, \hat{y}, \hat{t})$,

$$F_{\hat{t}} + \tfrac{17}{462}\nabla^4 F + \nabla^2 F - \mathrm{Di}(\nabla F)^2 + (\beta_b + \beta_t)F = 0. \tag{41}$$

Equation (41) is a damped version of the familiar Kuramoto-Sivashinsky equation [9,10], which often serves as a paradigmatic pattern-forming model for spatiotemporal chaos. Once we know the function F, the temperature field of the liquid layer is determined by

$$T = T_- + (T_- - T_+)(-z + \varepsilon F). \tag{42}$$

III. NUMERICAL EXPERIMENTS

Using the rescaling

$$F = \frac{1}{2\,\mathrm{Di}}\Phi, \quad \hat{x} = \sqrt{\frac{17}{231}}\xi, \quad \hat{y} = \sqrt{\frac{17}{231}}\eta, \quad \hat{t} = \frac{34}{231}\tau, \tag{43}$$

$$\beta_b + \beta_t = \frac{231}{34}\alpha,$$

we bring Eq. (41) to a single-parameter form, which is more convenient for numerical simulations,

$$\Phi_\tau + \nabla^4 \Phi + 2\nabla^2 \Phi - (\nabla \Phi)^2 + \alpha \Phi = 0. \tag{44}$$

Linear stability analysis of the trivial solution ($\Phi = 0$), corresponding to the absence of convection, yields the dispersion relation

$$\omega = 2k^2 - k^4 - \alpha. \tag{45}$$

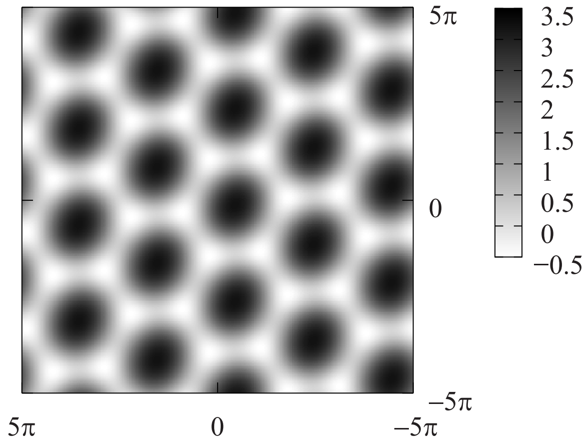

FIG. 1. Hexagonal cellular structure of the temperature field at $\alpha = 1$, with periodic boundary conditions at $\xi = \pm 5\pi$ or $\eta = \pm 5\pi$. Darker shading corresponds to higher levels of temperature.

Here ω is the instability growth rate and $k = \sqrt{p^2 + q^2}$, where p and q are the perturbation ($\delta\Phi$) wave numbers

$$\delta\Phi \sim \exp(ip\xi + iq\eta + \omega\tau). \tag{46}$$

The trivial solution $\Phi = 0$ is linearly stable or unstable depending on whether the heat loss parameter α is greater or less than unity.

The numerical solution of Eq. (44) shows that near the linear stability threshold ($\alpha = 1$) the convective flow assumes a time-independent regular hexagonal cellular structure (Fig. 1). Moreover, this pattern survives even for the values of α slightly above unity, indicating the supercritical nature of the bifurcation at $\alpha = 1$ (Fig. 2). At sufficiently small α the hexagonal structure transforms into an irregular patter of chaotically recombing cells (Fig. 3). The numerical method employed is outlined in the Appendix.

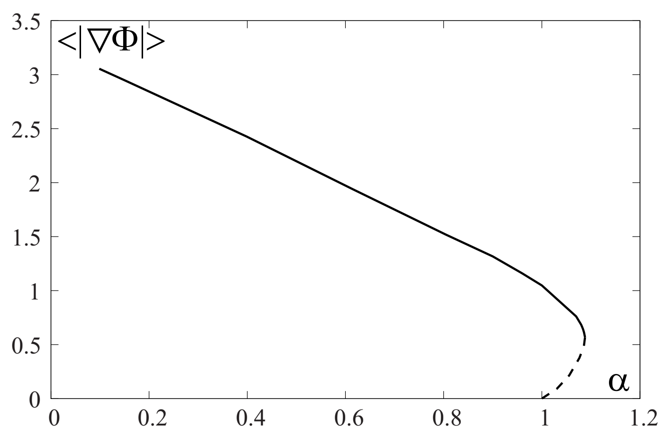

FIG. 2. Bifurcation diagram: spatial average $\langle|\nabla\Phi|^2\rangle$ vs α. The dashed line represents the expected unstable branch (see also Ref. [11]).

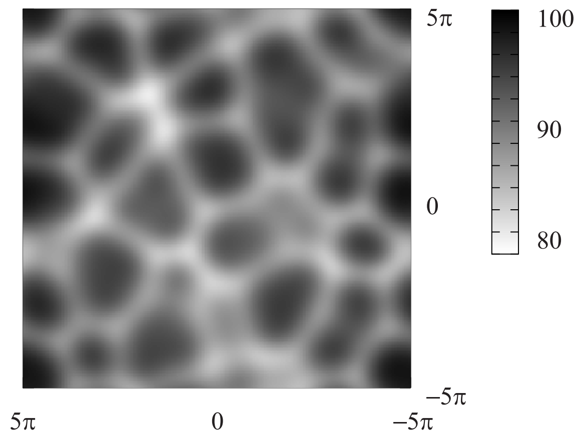

(a)

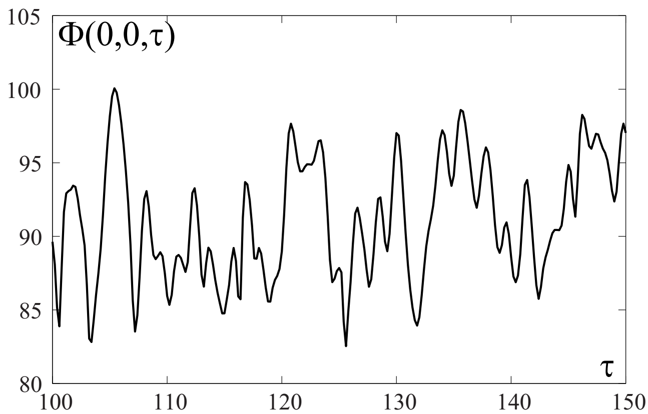

(b)

FIG. 3. (a) Irregular cellular structure of the temperature field at $\alpha = 0.1$. (b) Time record of $\Phi(0, 0, \tau)$. See also the caption for Fig. 1.

IV. CONCLUSION

The formulation in the present work employed rigid (nonslip) boundary conditions at $\hat{z} = 0, 1$ Eq. (7). One may also consider alternative rigid-free or free-free conditions where $\mathrm{Ra}_c = 320$ and 120, respectively, and where the second term of the F equation (41) becomes $\frac{58}{693}\nabla^4 F$ and $\frac{1091}{5544}\nabla^4 F$, respectively [see the appropriately rescaled Eq. (3.15) of Ref. [2]]. This change, however, does not affect the structure of the associated Φ equation (44).

At small viscous dissipation ($\mathrm{Di} \sim \varepsilon$) the equation for Φ may acquire other nonlinear terms, e.g., $\nabla[(\nabla\Phi)^2\nabla\Phi]$ and $\nabla[(\nabla^2\Phi)\nabla\Phi]$ [2,5], suppressed in the present analysis. This problem is of independent interest and is left for future discussion.

The two-dimensional Kuramoto-Sivashinsky equation has been extensively explored previously employing different numerical strategies (see, e.g., [11–14]). A fascinating animation of the emerging spatiotemporal dynamics was recently conducted by Richters-Finger using a pseudospectral scheme [15,16].

The present study is concerned with the asymptotic behavior close to the onset of convection. It would certainly be of interest to relax this restriction by direct numerical simulations of the model (1)–(8) augmented with some lateral (e.g., periodic) boundary conditions.

ACKNOWLEDGMENTS

This study was supported in part by the U.S.-Israel Bination Science Foundation (Grant No. 2020-005). P.V.G. was also supported in part by the Simons Foundation (Grant No. 317882). The numerical simulations were performed at the Computer Center of Tel Aviv University.

APPENDIX A: NUMERICAL SCHEME AND RESOLUTION TEST

The solution of Eq. (44) is sought by the finite-difference method over the square domain $-5\pi < \xi, \eta < 5\pi$ with cyclic boundary conditions on $\xi = \pm 5\pi$ or $\eta = \pm 5\pi$. The computational domain is covered with a uniform net with equal spatial steps $h_\xi = h_\eta = h$. Two rows of ghost points are added across each boundary for handling the boundary conditions.

Partial derivatives in ξ are approximated as

$$\frac{\partial \Phi}{\partial \xi} = \frac{\Phi_{n+1,m} - \Phi_{n-1,m}}{2h} + O(h^2), \tag{A1}$$

$$\frac{\partial^2 \Phi}{\partial \xi^2} = \frac{\Phi_{n+1,m} - 2\Phi_{n,m} + \Phi_{n-1,m}}{h^2} + O(h^2), \tag{A2}$$

$$\frac{\partial^4 \Phi}{\partial \xi^4} = \frac{\Phi_{n+2,m} - 4\Phi_{n+1,m} + 6\Phi_{n,m} - 4\Phi_{n-1,m} + \Phi_{n-2,m}}{h^4} + O(h^2). \tag{A3}$$

Partial derivatives in η are treated in a similar way.

The mixed partial derivative is approximated as

$$\frac{\partial^4 \Phi}{\partial \xi^2 \partial \eta^2} = \frac{1}{h^2}\left(\frac{\Phi_{n+1,m-1} - 2\Phi_{n,m-1} + \Phi_{n-1,m-1}}{h^2} - 2\frac{\Phi_{n+1,m} - 2\Phi_{n,m} + \Phi_{n-1,m}}{h^2} + \frac{\Phi_{n+1,m+1} - 2\Phi_{n,m+1} + \Phi_{n-1,m+1}}{h^2}\right) + O(h^2). \tag{A4}$$

Here n and m are net coordinates of the point (nh, mh), and $\Phi_{n,m} = \Phi(nh, mh)$.

The temporal derivative is handled by the explicit Euler method of the first order in $\Delta\tau$. If all spatial items of the finite-difference operator are of second order then the overall degree of approximation of the operator is 2 for the spatial step [17].

The resolution test is conducted following the recommendation and algorithm of Ref. [18]. Simulations with three different spatial steps $h_1 = h_0 = 0.1277$, $h_2 = h_0/\sqrt{2}$, and $h_3 = h_0/2$ were conducted; $h_1/h_2 = h_2/h_3 = \sqrt{2} > 1.3$ (see Ref. [18]). The results are presented in Table I.

The convergence rate is 2.17 [see Eq. (3) of Ref. [18]]. This value corresponds to the second degree of approximation of the finite-difference operator. The predicted value for the spatial average $\langle|\nabla\Phi|\rangle(h \to 0)$ is 1.05016. Errors

$$\frac{\langle|\nabla\Phi|\rangle(h) - \langle|\nabla\Phi|\rangle(h \to 0)}{\langle|\nabla\Phi|\rangle(h \to 0)} \tag{A5}$$

are shown in the last column of the Table I. The error, even for the minimal resolution, is small enough for our purposes. Simulations corresponding to Figs. 1–3 are carried out at $h = 0.1277$.

TABLE I. Results of the resolution test for $\alpha = 1$.

i	h_i	$\Delta\tau$	$\langle\|\nabla\Phi\|\rangle$	Error
1	0.1277	10^{-5}	1.04852	0.16%
2	0.08975	2.5×10^{-6}	1.04939	0.07%
3	0.06334	10^{-6}	1.04980	0.035%

[1] M. G. Velarde and R. Perez Cordon, On the (non-linear) foundations of boussinesq approximation applied to a thin layer of fluid. (II). Viscous dissipation and large cell gap effects, J. Phys. (Paris) **37**, 177 (1976).
[2] C. J. Chapman and M. R. E. Proctor, Nonlinear Rayleigh-Bénard convection between poorly conducting boundaries, J. Fluid Mech. **101**, 759 (1980).
[3] C. J. Chapman, S. Childress, and M. R. E. Proctor, Long wavelength thermal convection between non-conducting boundaries, Earth Planet. Sci. Lett. **51**, 362 (1980).
[4] J. M. Hewitt, D. P. McKenzie, and N. O. Weiss, Large aspect ratio cells in two-dimensional thermal convection, Earth Planet. Sci. Lett. **51**, 370 (1980).
[5] V. L. Gertsberg and G. I. Sivashinsky, Large cells in nonlinear Rayleigh-Bénard convection, Prog. Theor. Phys. **66**, 1219 (1981).
[6] S. M. Cox, The onset of thermal convection between poorly conducting horizontal boundaries in the presence of a shear flow, SIAM J. Appl. Math. **56**, 1317 (1996).
[7] Lord Rayleigh, On convection currents in a horizontal layer of fluid, when the higher temperature is on the upper side, Philos. Mag. **32**, 529 (1916).
[8] F. H. Busse and N. Riahi, Nonlinear convection in a layer with nearly insulating boundaries, J. Fluid Mech. **96**, 243 (1980).
[9] Y. Kuramoto and T. Tsuzuki, Persistent propagation waves in dissipative media far from thermal equilibrium, Prog. Theor. Phys. **55**, 356 (1976).
[10] G. I. Sivashinsky, Nonlinear analysis of hydrodynamic instability in laminar flames—I. Derivation of basic equations, Acta Astronaut. **4**, 1177 (1977).
[11] L. Shtilman and G. Sivashinsky, On the hexagonal structure of cellular flames, Can. J. Phys. **68**, 768 (1990).
[12] H. Gomez and J. Paris, Numerical simulation of asymptotic states of the damped Kuramoto-Sivashinsky equation, Phys. Rev. E **83**, 046702 (2011).
[13] A. Kalogirou, E. E. Keaveng, and D. T. Papageorgiou, An in-depth numerical study of the two-dimensional Kuramoto-Sivashinsky equation, Proc. R. Soc. A **471**, 20140932 (2015).
[14] M. Dehghan and V. Mohammadi, Two-dimensional simulation of the damped Kuramoto-Sivashinsky equation via radial basis function-generated finite difference scheme combined with an exponential time discretization, Eng. Anal. Boundary Elem. **107**, 168 (2019).
[15] S. Richters-Finger, Kuramoto-Sivashinsky equation: Spatiotemporal chaos, YouTube, https://www.youtube.com/watch?v=OWYz3bVKl6k (2019).
[16] S. Richters-Finger, Damped Kuramoto-Sivashinsky equation: Hexagonal pattern, YouTube, https://www.youtube.com/watch?v=40G8CUyRKH8 (2019).
[17] D. A. Anderson, J. C. Tannehill, and R. H. Pletcher, *Computational Fluid Mechanics and Heat Transfer* (Hemisphere, New York, 1984).
[18] I. B. Celik, U. Ghia, P. J. Roache, C. J. Freitas, H. Coleman, and P. E. Raad, Procedure for estimation and reporting of uncertainty due to discretization in CFD applications, J. Fluid. Eng. **130**, 078001 (2008).